

DEDICATED SUPERNOVA DETECTION BY A NETWORK OF NEUTRAL CURRENT SPHERICAL TPC'S.

J.D. Vergados*

RCNP, Osaka University, Ibaraki 567-0047, Japan.[†]

Y. Giomataris[‡]

CEA, Saclay, DAPNIA, Gif-sur-Yvette, Cedex, France

(Dated: August 6, 2018)

Supernova neutrinos can easily be detected by a spherical gaseous TPC detector measuring very low energy nuclear recoils. The expected rates are quite large for a neutron rich target since the neutrino nucleus neutral current interaction yields a coherent contribution of all neutrons. As a matter of fact for a typical supernova at 10 kpc, about 1000 events are expected using a spherical detector of radius 4 m with Xe gas at a pressure of 10 Atm. A world wide network of several such simple, stable and low cost supernova detectors with a running time of a few centuries is quite feasible.

PACS numbers: 13.15.+g, 14.60Lm, 14.60Bq, 23.40.-s, 95.55.Vj, 12.15.-y.

I. INTRODUCTION

Neutrinos appear to be excellent probes for studying the deep sky. They travel large distances with the speed of light. They can pass through obstacles, without getting distorted on their way and they are not affected by the presence of magnetic fields. Thus with neutrinos one can see much further than with light. With light one cannot observe further than 50 Mpc (1 Mpc=3.3x10⁶ light years). Furthermore the detection of neutrinos reveals information about the source and more specifically about the source interior. Without neutrinos we would probably know nothing about the sun's interior. Thus neutrinos offer a good hope for understanding the early stages of a supernova. In a typical supernova an energy of about 10⁵³ ergs is released in the form of neutrinos [1],[2]. These neutrinos are emitted within an interval of about 10 s after the explosion and they travel to Earth undistorted, except that, on their way to Earth, they may oscillate into other flavors. The phenomenon of neutrino oscillations is by now established by the observation of atmospheric neutrino oscillations [3] interpreted as $\nu_\mu \rightarrow \nu_\tau$ oscillations, as well as ν_e disappearance in solar neutrinos [4]. These results have been recently confirmed by the KamLAND experiment [5], which exhibits evidence for reactor antineutrino disappearance. Thus for traditional detectors relying on the charged current interactions the precise event rate may depend critically on the specific properties of the neutrinos. The time integrated spectra in the case of charged current detectors, like the SNO experiment, depend on the neutrino oscillations [6]. This, of course, may turn into an advantage for the study of

the neutrino properties [7]. An additional problem is the fact that the charged current cross sections depend on the details of the structure of the nuclei involved.

During the last years various detectors aiming at detecting recoiling nuclei have been developed in connection with dark matter searches [8] with thresholds in the 10 keV region. Recently, however, it has become feasible to detect neutrinos by measuring the recoiling nucleus and employing gaseous detectors with much lower threshold energies. Thus one is able to explore the advantages offered by the neutral current interaction, exploring ideas put forward more than a decade ago [9]. This way the deduced neutrino fluxes do not depend on the neutrino oscillation parameters (e.g. the mixing angles). Even in our case, however, the obtained rates depend on the assumed characteristic temperature for each flavor, see sec. VI. Furthermore this interaction, through its vector component, can lead to coherence, i.e. an additive contribution of all nucleons in the nucleus. Since the vector contribution of the protons is tiny, the coherence is mainly due to the neutrons of the nucleus.

In this paper we will derive the amplitude for the differential neutrino nucleus coherent cross section. Then we will utilize the available information regarding the energy spectrum of supernova neutrinos and estimate the expected number of events for all the noble gas targets. We will show that these results can be exploited by a network of small and relatively cheap spherical TPC detectors placed in various parts of the world (for a description of the apparatus see our earlier work [10]). The operation of such devices as a network will minimize the background problems. There is no need to go underground, but one may have to go sufficiently deep underwater to balance the high pressure of the gas target. Other types of detectors have also been proposed [11],[12].

Large gaseous volumes are easily obtained by employing long drift technology (i.e TPC) that can provide massive targets by increasing the gas pressure. Combined with an adequate amplifying structure and low energy thresh-

*Electronic address: vergados@cc.uoi.gr

[†]Physics Department, University of Ioannina, Ioannina, Greece.

[‡]Electronic address: ioa@hep.saclay.cea.fr

olds, a three-dimensional reconstruction of the recoiling particle, electron or nucleus, can be obtained. The use of new micropattern detectors and especially the novel Micromegas [13] provide excellent spatial and time accuracy that is a precious tool for pattern recognition and background rejection [14],[15]. The virtue of using such large gaseous volumes and the new high precision microstrip gaseous detectors has been recently discussed in a dedicated workshop [16] and their relevance for low energy neutrino physics and dark matter detection has been widely recognized. Such low-background low-energy threshold systems are actually successfully used in the CAST [17], the solar axion experiment, and are under development for several low energy neutrino or dark matter projects [10],[18].

II. THE NOSTOS DETECTOR NETWORK

Before we embark on our calculations involving the event rates for supernova neutrino detection of a gaseous TPC detector we like to spend a little time in discussing the detector. A description of the NOSTOS project and details of the spherical TPC detector are given in [10] and is shown in 1. We have built a spherical prototype

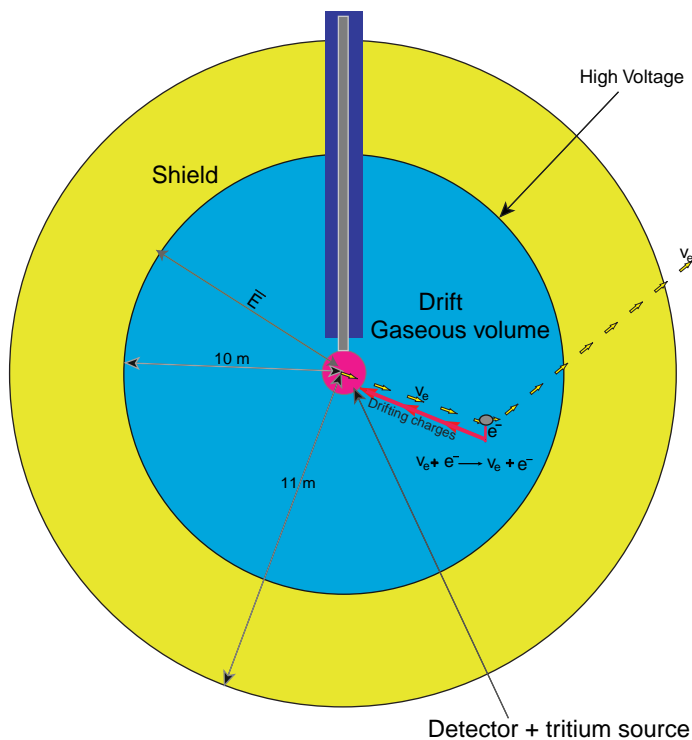


FIG. 1: A sketch of the NOSTOS detector drawn originally for detecting very low energy electron recoils. The corresponding one for detection of nuclear recoils is analogous.

1.3 m in diameter which is described in [29] (see Fig. 2) . The outer vessel is made of pure Cu (6 mm thick)

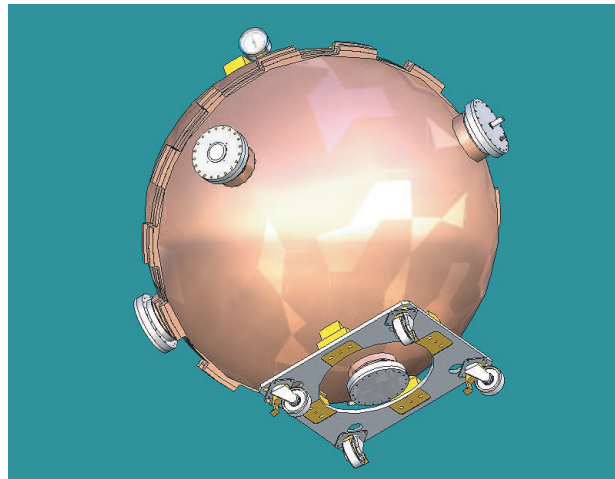


FIG. 2: First prototype - The SACLAY sphere: $R = 1.3$ m, $V = 1$ m³, spherical vessel of Cu 6 mm thick, pressure up to 5 bar (already tested up to 1.5 bar), vacuum tight, 10⁻⁶ mbar (outgassing $\sim 10^9$ mbar/s)

allowing to sustain pressures up to 5 bar. The inner detector is just a small sphere, 10 mm in diameter, made of stainless steel as a proportional counter located at the center of curvature of the TPC. We intend to use as amplifying structure a spherical TPC [30] and developments are currently under way to build a spherical TPC detector using new technologies. First tests were performed by filling the volume with argon mixtures and are quite promising. High gains are easily obtained and the signal to noise is large enough for sub-keV threshold. The whole system looks stable and robust. The advantages of using the spherical detector concept are the following;

1. The natural radial focusing of the TPC allows to collect and amplify the deposited charges by a simple and robust detector using a single electronic channel to read out a large gaseous volume. The small size associated to small detector capacitance permits one to achieve very low electronic noise. In the present prototype the noise is as low as a few hundred electrons and has easily been obtained; with optimized low noise amplifiers we hope to lower it to the level of a few tenths. This is a key point for the obtaining a very low energy threshold, i.e. down to 100 eV, by operating the detector at moderate gain of about 100. Such low gains are easily obtained at atmospheric pressure and open the way to operate the TPC at high pressures. We target to achieve pressures as high as 10 bar for Xenon gas. Even higher pressures by a factor 3-6 are aimed at in the case of Argon gas in order to achieve, to first order, the same number of events.
2. The radial electric field, inversely proportional to the square of the radius, is a crucial point for mea-

suring the depth of the interaction by a simple analysis of the time structure of the detector signal. A position resolution of about 10 cm has been already obtained, a fact that is of paramount importance for improving the time resolution of the detector and rejecting background events by applying fiducial cuts.

3. Building a high pressure metallic sphere, for instance made out of stainless steel or copper, seems to assure an excellent quality of the gas mixture and turns out that a single gas filling with pure gas is sufficient to maintain the stability of the signal for several months. We are pushing the technology to improve the properties of the various elements in order to achieve stability over many years.
4. Big high pressure-secure tanks are under development by many international companies for hydrogen or oil storage, and therefore the main element of the TPC could be shipped at moderate cost.

Our idea is then to build several such low cost and robust detectors and install them in several places over the world. First estimations show that the required background level is modest and therefore there is no need for a deep underground laboratory. A mere 100 meter water equivalent coverage seems to be sufficient to reduce the cosmic muon flux at the required level (in the case of many such detectors in coincidence, a modest shield is sufficient). The maintenance of such system could be easily assured by Universities or even by secondary schools. Thanks to the simplicity of the system it could be operated by young students with a specific running program and simple maintenance every a few years. Notice that such detector scheme, measuring low energy nuclear recoils from neutrino nucleus elastic scattering, do not determine the incident neutrino vector and, therefore, it is not possible this way to localize the Supernova. A cluster of such detectors in coincidence, however, could localize the star by a triangulation technique.

A network of such detectors in coincidence with a sub-keV threshold could also be used to observe unexpected low energy events. This low energy range has never been explored using massive detectors. A challenge of great importance will be the synchronization of such a detector cluster with the astronomical γ -ray burst telescopes to establish whether low energy recoils are emitted in coincidence with the mysterious γ bursts.

III. STANDARD AND NON STANDARD WEAK INTERACTION

The standard neutral current left handed weak interaction can be cast in the form:

$$\mathcal{L}_{\Pi} = -\frac{G_F}{\sqrt{2}} [\bar{\nu}_\alpha \gamma^\mu (1 - \gamma^5) \nu_\alpha] [\bar{q} \gamma_\mu (g_V(q) - g_A(q) \gamma^5) q] \quad (1)$$

(diagonal in flavor space) with

$$\begin{aligned} g_V(u) &= \frac{1}{2} - \frac{4}{3} \sin^2 \theta_W, & g_A(u) &= \frac{1}{2}; \\ g_V(d) &= -\frac{1}{2} + \frac{2}{3} \sin^2 \theta_W, & g_A(d) &= -\frac{1}{2} \end{aligned} \quad (2)$$

At the nucleon level we get:

$$\mathcal{L}_{\Pi} = -\frac{G_F}{\sqrt{2}} [\bar{\nu}_\alpha \gamma^\mu (1 - \gamma^5) \nu_\alpha] [\bar{N} \gamma_\mu (g_V(N) - g_A(N) \gamma^5) N] \quad (3)$$

with

$$\begin{aligned} g_V(p) &= \frac{1}{2} - 2 \sin^2 \theta_W, & g_A(p) &= 1.27 \frac{1}{2}; \\ g_V(n) &= -\frac{1}{2}, & g_A(n) &= -1.27 \frac{1}{2} \end{aligned} \quad (4)$$

Beyond the standard level one has further interactions which need not be diagonal in flavor space. Thus

$$\begin{aligned} g_V(q) - g_A(q) \gamma^5 &\rightarrow \\ (g_V^{SM}(q) - g_A^{SM}(q) \gamma^5) \delta_{\alpha\beta} &+ (\lambda^{qL} \delta_{\alpha\beta} + \epsilon_{\alpha\beta}^{qL}) (1 - \gamma^5) \\ [\bar{\nu}_\alpha \gamma^\mu (1 - \gamma^5) \nu_\alpha] &\rightarrow [\bar{\nu}_\alpha \gamma^\mu (1 - \gamma^5) \nu_\beta] \end{aligned} \quad (5)$$

Furthermore at the nucleon level

$$\begin{aligned} g_V(N) - g_A(N) \gamma^5 &\rightarrow (g_V^{SM}(N) - g_A^{SM}(N) \gamma^5) \delta_{\alpha\beta} \\ &+ (\lambda^{NL} \delta_{\alpha\beta} + \epsilon_{\alpha\beta}^{NL}) (1 - 1.27 \gamma^5) \\ [\bar{\nu}_\alpha \gamma^\mu (1 - \gamma^5) \nu_\alpha] &\rightarrow [\bar{\nu}_\alpha \gamma^\mu (1 - \gamma^5) \nu_\beta] \end{aligned} \quad (6)$$

with

$$\begin{aligned} \lambda^{pL} &= 2\lambda^{uL} + \lambda^{dL}, & \lambda^{nL} &= \lambda^{dL} + 2\lambda^{uL}, \\ \epsilon_{\alpha\beta}^{pL} &= 2\epsilon_{\alpha\beta}^{uL} + \epsilon_{\alpha\beta}^{dL}, & \epsilon_{\alpha\beta}^{nL} &= \epsilon_{\alpha\beta}^{uL} + 2\epsilon_{\alpha\beta}^{dL} \end{aligned} \quad (7)$$

In the above expressions λ^{qL} can arise, e.g., from radiative corrections, see e.g. PDG [19] and $\epsilon_{\alpha\beta}^{qL}$ from R-parity violating interactions in supersymmetric models [20]-[21]. Indeed since R-parity conservation has no robust theoretical motivation one may accept an extended framework of the MSSM with R-parity non-conservation MSSM. In this case the superpotential W acquires additional R-parity violating terms:

$$\begin{aligned} W_{R_p} &= \lambda_{ijk} L_i L_j E_k^c + \lambda'_{ijk} L_i Q_j D_k^c \\ &+ \lambda''_{ijk} U_i^c D_j^c D_k^c + \mu_j L_j H_u \end{aligned} \quad (8)$$

Of interest to us here is the $\lambda'_{ijk} L_i Q_j D_k^c$ involving first generation quarks and s-quarks, i.e the term $\lambda'_{\alpha 11} L_\alpha Q_1 D_1^c$. From this term in four component notation we get the contribution

$$\lambda'_{\alpha 11} (\bar{d}_R^c \nu_{\alpha L} - \bar{u}_R^c \alpha_L) \tilde{d}^c, \quad \alpha = e, \mu, \tau$$

where $\nu_{\alpha L} = \frac{1}{2}(1 - \gamma_5)\nu_\alpha$ etc. Thus

- The first term at tree level yields the interaction

$$-\frac{\lambda'_{\alpha 11}\lambda'_{\beta 11}}{m_{d_L}^2}\bar{\nu}_{\alpha L}d_R^c\bar{d}_R^c\nu_{\beta L} \quad (9)$$

By performing a Fierz transformation we can rewrite it in the form:

$$\frac{1}{2}\frac{\lambda'_{\alpha 11}\lambda'_{\beta 11}}{m_{d_L}^2}\bar{\nu}_{\alpha L}\gamma^\mu\nu_{\beta L}\bar{d}_R^c\gamma_\mu d_R^c \quad (10)$$

The previous equation can be cast in the form:

$$\begin{aligned} \mathcal{L}_d &= -\frac{G_F}{\sqrt{2}}\epsilon_{\alpha\beta}^d[\bar{\nu}_\alpha\gamma^\mu(1-\gamma^5)\nu_\beta][\bar{d}\gamma_\mu(1-\gamma^5)d]; \\ \epsilon_{\alpha\beta}^d &= \lambda'_{\alpha 11}\lambda'_{\beta 11}\frac{m_W^2}{m_{d_L}^2} \end{aligned} \quad (11)$$

There is no such term associated with the u quark, $\epsilon_{\alpha\beta}^u = 0$.

- Proceeding in an analogous fashion the collaborative effect of the first and second term, for $\alpha, \beta = e, \mu, \tau$, yields the charged current contribution:

$$\mathcal{L}_{du} = \frac{G_F}{\sqrt{2}}\epsilon_{\alpha\beta}^d[\bar{\alpha}\gamma^\mu(1-\gamma^5)\nu_\beta][\bar{u}\gamma_\mu(1-\gamma^5)d] \quad (12)$$

- Finally the second term, for $\alpha, \beta = e, \mu, \tau$, leads to a neutral current contribution of the charged leptons:

$$\mathcal{L}_u = \frac{G_F}{\sqrt{2}}\epsilon_{\alpha\beta}^d[\bar{\alpha}\gamma^\mu(1-\gamma^5)\beta][\bar{u}\gamma_\mu(1-\gamma^5)u] \quad (13)$$

The above non standard flavor changing neutral current interaction have been found to play an important role in the infall stage of a stellar collapse [23]. Furthermore precise measurements involving the neutral current neutrino-nucleus interactions may yield valuable information about the non standard interactions [24]. They are not, however, going to be further considered in this work.

IV. ELASTIC NEUTRINO NUCLEON SCATTERING

The cross section for elastic neutrino nucleon scattering has extensively been studied. It has been shown that at low energies the weak differential cross section can be simplified and be cast in the form: [1],[22]:

$$\begin{aligned} \left(\frac{d\sigma}{dT_N}\right)_w &= \frac{G_F^2 m_N}{2\pi}[(g_V + g_A)^2 \\ &+ (g_V - g_A)^2\left[1 - \frac{T_N}{E_\nu}\right]^2 + (g_A^2 - g_V^2)\frac{m_N T_N}{E_\nu^2}] \end{aligned} \quad (14)$$

where m_N is the nucleon mass and g_V, g_A are the weak coupling constants. Neglecting their dependence on the

momentum transfer to the nucleon they take the form (see previous section):

$$g_V = -2\sin^2\theta_W + 1/2 \approx 0.04, \quad g_A = \frac{1.27}{2}, \quad (\nu, p) \quad (15)$$

$$g_V = -1/2, \quad g_A = -\frac{1.27}{2}, \quad (\nu, n) \quad (16)$$

In the above expressions for the axial current the renormalization in going from the quark to the nucleon level was taken into account. For antineutrinos $g_A \rightarrow -g_A$. To set the scale we write:

$$\frac{G_F^2 m_N}{2\pi} = 5.14 \times 10^{-41} \frac{\text{cm}^2}{\text{MeV}} \quad (17)$$

The nucleon energy depends on the neutrino energy and the scattering angle, the angle between the direction of the recoiling particle and that of the incident neutrino. In the laboratory frame it is given by:

$$T_N = \frac{2m_N(E_\nu \cos\theta)^2}{(m_N + E_\nu)^2 - (E_\nu \cos\theta)^2}, \quad 0 \leq \theta \leq \pi/2 \quad (18)$$

(forward scattering). For sufficiently small neutrino energies, the last equation can be simplified as follows:

$$T_N \approx \frac{2(E_\nu \cos\theta)^2}{m_N}$$

The above formula can be generalized to any target and can be written in dimensionless form as follows:

$$y = \frac{2\cos^2\theta}{(1+1/x_\nu)^2 - \cos^2\theta}, \quad y = \frac{T_{recoil}}{m_{recoil}}, \quad x_\nu = \frac{E_\nu}{m_{recoil}} \quad (19)$$

The maximum energy occurs when $\theta = 0$, $y_{max} = \frac{2}{(1+1/x_\nu)^2 - 1}$, in agreement with Eq. (2.5) of ref. [1]. This relationship is plotted in Fig. 3. One can invert Eq. 19

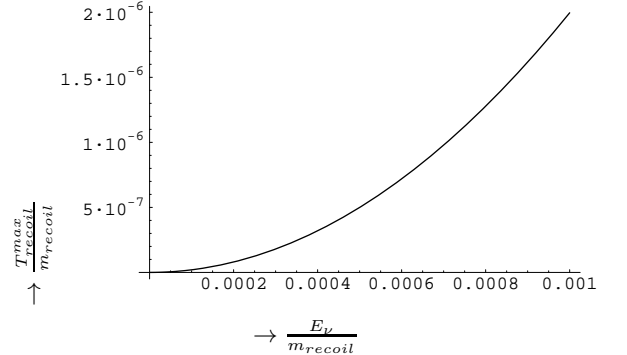


FIG. 3: The maximum recoil energy as a function of the neutrino energy (both in units of the recoiling mass). The scale is realistic for nuclear recoils of the type of experiments considered here.

and get the neutrino energy associated with a given recoil energy and scattering angle. One finds

$$x_\nu = \left[-1 + \cos\theta \sqrt{1 + \frac{2}{y}} \right]^{-1}, \quad 0 \leq \theta \leq \pi/2 \quad (20)$$

The minimum neutrino energy for a give recoil energy is given by:

$$x_\nu^{min} = \left[-1 + \sqrt{1 + \frac{2}{y}} \right]^{-1} = \frac{y}{2} \left(1 + \sqrt{1 + \frac{2}{y}} \right) \quad (21)$$

in agreement with Eq. (4.2) of ref. [1]. The last equation is useful in obtaining the differential cross section (with respect to the recoil energy) after folding with the neutrino spectrum and it is shown in Fig. 4

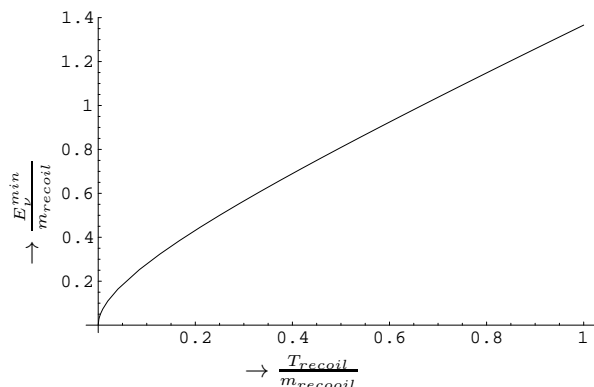


FIG. 4: The minimum neutrino energy as a function of the recoil energy (both in units of the recoiling mass). The scale is not realistic for nuclear recoils considered here, but relevant for other experiments. The realistic scale for experiments considered here can be deduced from Fig. 3 by exchanging the coordinate axes.

V. COHERENT NEUTRINO NUCLEUS SCATTERING

From the above expressions we see that the vector current contribution, which may lead to coherence, is negligible in the case of the protons. Thus the coherent contribution [25] may come from the neutrons and is expected to be proportional to the square of the neutron number. The neutrino-nucleus scattering can be obtained from the amplitude of the neutrino nucleon scattering under the following assumptions:

- Employ the appropriate kinematics, i.e. those involving the elastically scattered nucleus.
- Ignore effects of the nuclear form factor. Such effects, which are not expected to be very large, are currently under study and they will appear elsewhere.

- The effective neutrino-nucleon amplitude is obtained as above with the substitution

$$\mathbf{q} \Rightarrow \frac{\mathbf{p}}{A}, \quad E_N \Rightarrow \sqrt{m_N^2 + \frac{\mathbf{p}^2}{A^2}} = \frac{E_A}{A}$$

with \mathbf{q} the nucleon momentum and \mathbf{p} the nuclear momentum.

Under the above assumptions the neutrino-nucleus cross section takes the form:

$$\begin{aligned} \left(\frac{d\sigma}{dT_A} \right)_w &= \frac{G_F^2 A m_N}{2\pi} \times \\ &[(M_V + M_A)^2 \left(1 + \frac{A-1}{A} \frac{T_A}{E_\nu} \right) \\ &+ (M_V - M_A)^2 \left(1 - \frac{T_A}{E_\nu} \right)^2 \left(1 - \frac{A-1}{A} \frac{T_A}{m_N} \frac{1}{E_\nu/T_A - 1} \right) \\ &+ (M_A^2 - M_V^2) \frac{A m_N T_A}{E_\nu^2}] \quad (22) \end{aligned}$$

Where M_V and M_A are the nuclear matrix elements associated with the vector and the axial current respectively and T_A is the energy of the recoiling nucleus. The axial current contribution vanishes for $0^+ \Rightarrow 0^+$ transitions. Anyway it is negligible in front of the coherent scattering due to neutrons. Thus the previous formula is reduced to:

$$\begin{aligned} \left(\frac{d\sigma}{dT_A} \right)_w &= \frac{G_F^2 A m_N}{2\pi} (N^2/4) F_{coh}(A, T_A, E_\nu), \\ F_{coh}(A, T_A, E_\nu) &= \left(1 + \frac{A-1}{A} \frac{T_A}{E_\nu} \right) + \left(1 - \frac{T_A}{E_\nu} \right)^2 \\ &\left(1 - \frac{A-1}{A} \frac{T_A}{m_N} \frac{1}{E_\nu/T_A - 1} \right) - \frac{A m_N T_A}{E_\nu^2} \quad (23) \end{aligned}$$

The function $F_{coh}(A, T_A, E_\nu)$ is shown in Fig 5 as a function of the recoil energy in the case of Ar (N=22) and Xe (N=77) for 10, 20, 30 and 40 MeV respectively. We see two reasons for enhancement of the cross section:

- The overall A factor due to the kinematics, which is counteracted by the smaller nuclear recoil energy when compared to the nucleon recoil energy for the same neutrino energy. This factor will be absorbed into the energy integrals, see the function $F_{fold}(A, T, (T_A)_{th})$ below.
- The N^2 enhancement due to coherence.

VI. SUPERNOVA NEUTRINOS

The number of neutrino events for a given detector depends on the neutrino spectrum and the distance of the source. We will consider a typical case of a source which is about 10 kpc, i.e. $D = 3.1 \times 10^{22}$ cm (of the order of the radius of the galaxy) with an energy output

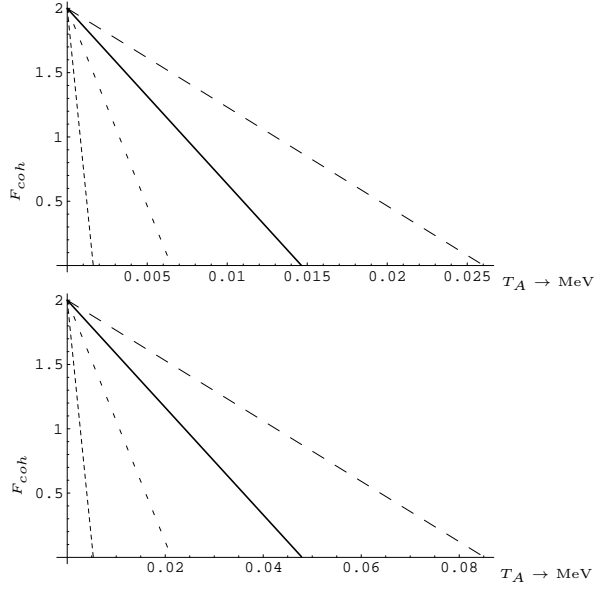


FIG. 5: The function $F_{coh}(A, T_A, E_\nu)$ as a function of the recoil energy T_A for, from left to right, $E_\nu = 10, 20, 30, 40$ MeV. The results shown are for Xe on the top and Ar at the bottom

of 3×10^{53} ergs with a duration of about 10 s. The neutrino spectra are parametrized as follows:

$$\frac{dN}{dE_{\nu_i}} = \frac{\Phi_i}{\langle E_i \rangle} \frac{\beta_i^{\beta_i}}{\Gamma(\beta_i)} \left(\frac{E_i}{\langle E_i \rangle} \right)^{\beta_i-1} \text{Exp} \left(-\beta_i \frac{E_i}{\langle E_i \rangle} \right) \quad (24)$$

where $\langle E_i \rangle$ is the average energy of neutrino flavor i with $E_{\nu_e} < E_{\tilde{\nu}_e} < E_{\nu_x}(E_{\tilde{\nu}_x})$ for $x = \mu, \tau$. The parameters Φ_i , $\langle E_i \rangle$ and β_i for each flavor, $\nu_e, \tilde{\nu}_e, \nu_x(\tilde{\nu}_x)$ with $x = \mu, \tau$ are determined phenomenologically [27]. In the present paper, in order to minimize the number of parameters, we will assume for simplicity that each neutrino flavor is characterized by a Fermi-Dirac like distribution times its characteristic cross section, which is adequate for our purposes. Thus:

$$\frac{dN}{dE_\nu} = \sigma(E_\nu) \frac{E_\nu^2}{1 + \exp(E_\nu/T)} = \frac{\Lambda}{JT} \frac{x^4}{1 + e^x}, \quad x = \frac{E_\nu}{T} \quad (25)$$

with $J = \frac{31\pi^6}{252}$, Λ a constant and T the temperature of the emitted neutrino flavor. Each flavor is characterized by its own temperature as follows:

$$T = 8 \text{ MeV for } \nu_\mu, \nu_\tau, \tilde{\nu}_\mu, \tilde{\nu}_\tau, T = 5 \text{ (3.5) MeV for } \tilde{\nu}_e (\nu_e)$$

The constant Λ is determined by the requirement that the distribution yields the total energy of each neutrino species.

$$U_\nu = \frac{\Lambda T}{J} \int_0^\infty dx \frac{x^5}{1 + e^x} \Rightarrow \Lambda = \frac{U_\nu}{T}$$

We will further assume that $U_\nu = 0.5 \times 10^{53}$ ergs per neutrino flavor. Thus one finds:

$$\Lambda = 0.89 \times 10^{58} (\nu_e), 0.63 \times 10^{58} (\tilde{\nu}_e), 0.39 \times 10^{58} (\text{other})$$

The emitted neutrino spectrum is shown in Fig. 6. The

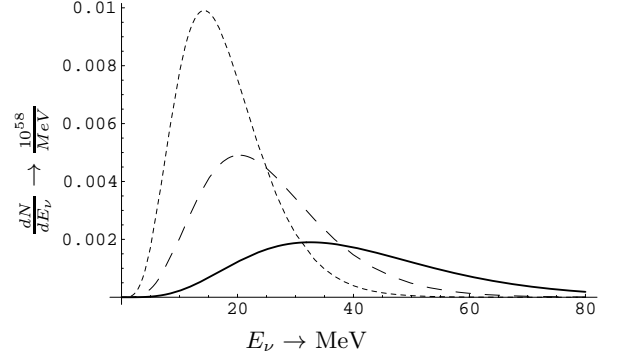


FIG. 6: The supernova neutrino spectrum. The short dash, long dash and continuous curve correspond to $\nu_e, \tilde{\nu}_e$ and all other flavors respectively

differential event rate (with respect to the recoil energy) is proportional to the quantity:

$$\frac{dR}{dT_A} = \frac{\lambda(T)}{J} \int_0^\infty dx F_{coh}(A, T_A, xT) \frac{x^4}{1 + e^x} \quad (26)$$

with $\lambda(T) = (0.89, 0.63, 0.39)$ for $\nu_e, \tilde{\nu}_e$ and all other flavors respectively. This is shown in Figs. 7 and 7. The total number of expected events for each neutrino species can be cast in the form:

$$\text{No of events} = \tilde{C}_\nu(T) h(A, T, (T_A)_{th}), \quad (27)$$

$$h(A, T, (T_A)_{th}) = \frac{F_{fold}(A, T, (T_A)_{th})}{F_{fold}(40, T, (T_A)_{th})} \quad (28)$$

with

$$F_{fold}(A, T, (T_A)_{th}) = \frac{A}{J} \int_{(T_A)_{th}}^{(T_A)_{max}} \frac{dT_A}{1 \text{ MeV}} \times \int_0^\infty dx F_{coh}(A, T_A, xT) \frac{x^4}{1 + e^x} \quad (29)$$

and

$$\tilde{C}_\nu(T) = \frac{G_F^2 m_N 1 \text{ MeV} N^2}{2\pi} \frac{1}{4} \Lambda(T) \frac{1}{4\pi D^2} \frac{PV}{kT_0} \quad (30)$$

Where k is Boltzmann's constant, P the pressure, V the volume, and T_0 the temperature of the gas.

Summing over all the neutrino species we can write:

$$\text{No of events} = C_\nu r(A) \frac{K(A, (T_A)_{th})}{K(40, (T_A)_{th})} Qu(A) \quad (31)$$

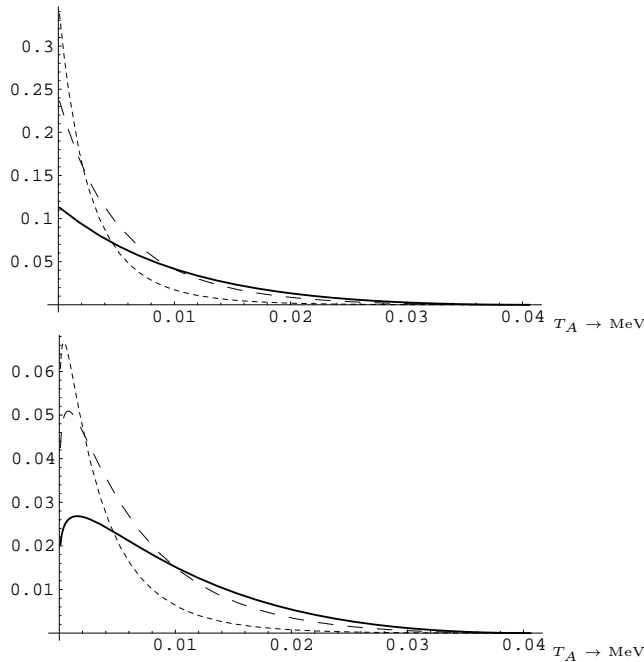


FIG. 7: The differential event rate as a function of the recoil energy T_A , in arbitrary units, for Xe. On the top we show the results without quenching, while at the bottom the quenching factor is included. We notice that the effect of quenching is more prevalent at low energies. The notation for each neutrino species is the same as in Fig. 6

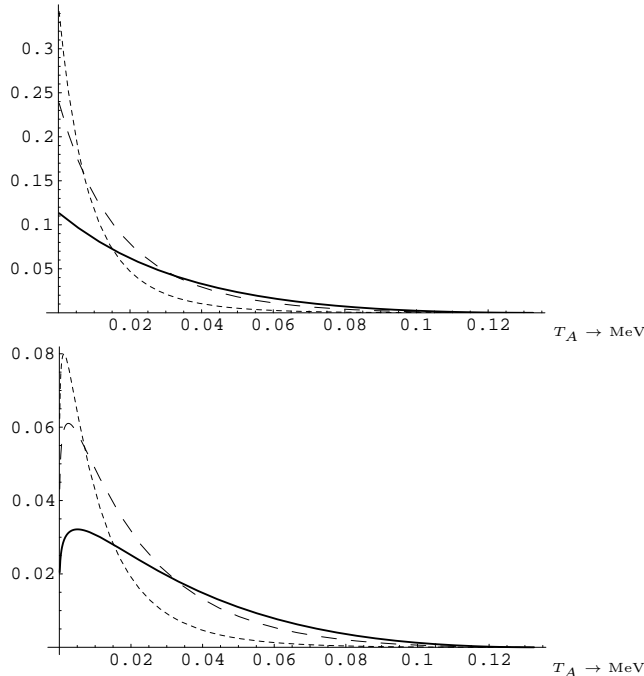


FIG. 8: The same as in Fig. 7 for the Ar target.

with

$$C_\nu = 153 \left(\frac{N}{22} \right)^2 \times \frac{U_\nu}{0.5 \times 10^{53} \text{ergs}} \left(\frac{10 \text{kpc}}{D} \right)^2 \frac{P}{10 \text{Atm}} \left[\frac{R}{4m} \right]^3 \frac{300}{T_0} \quad (32)$$

In the above expression $r(A)$ is a kinematical parameter depending on the nuclear mass number, which is essentially unity.

$K(A, (T_A)_{th})$ is the rate at a given threshold energy divided by that at zero threshold. It depends on the threshold energy, the assumed quenching factor and the nuclear mass number. It is unity at $(T_A)_{th} = 0$. The function $r(A)$ is plotted in 9. It is seen that it can be well approximated by unity.

From the above equation we find that, ignoring quenching, the following expected number of events:

$$1.25, 31.6, 153, 614, 1880 \text{ for He, Ne, Ar, Kr and Xe} \quad (33)$$

respectively. For other possible targets the rates can be found by the above formulas or interpolation.

The function $K(A, (T_A)_{th})$ is plotted in Fig. 10 for

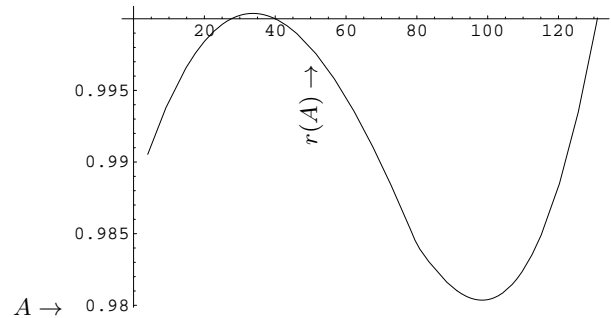


FIG. 9: The function $r(A)$ versus the nuclear mass number. To a good approximation $r(A) \simeq 1.0$ (for definitions see text)

threshold energies up to 2keV. We see that the threshold effects are stronger in heavier systems since, on the average, the transferred energy is smaller. Thus for a threshold energy of 2 keV in the case of Xe the number of events is reduced by 30% compared to those at zero threshold. The quantity $Qu(A)$ is a factor less than one multiplying the total rate, assuming a threshold energy $(T_A)_{th} = 100\text{eV}$, due to the quenching. The idea of quenching is introduced, since, for low energy recoils, only a fraction of the total deposited energy goes into ionization. The ratio of the amount of ionization induced in the gas due to nuclear recoil to the amount of ionization induced by an electron of the same kinetic energy is referred to as a quenching factor Q_{fac} . This factor depends mainly on the detector material, the recoiling energy as well as the process considered [26]. In our estimate of $Qu(T_A)$ we assumed a quenching factor of the following empirical form

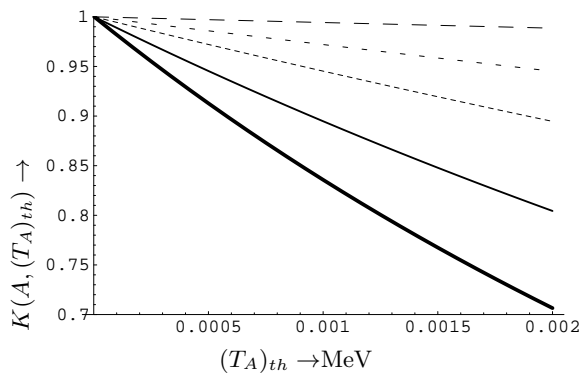


FIG. 10: The function $K(A, (T_A)_{th})$ versus $(T_A)_{th}$ for various nuclear mass numbers without the quenching factor. From top to bottom He, Ne, Ar, Kr and Xe. (for definitions see text)

motivated by the Lidhard theory [26]-[28]:

$$Q_{fac}(T_A) = r_1 \left[\frac{T_A}{1keV} \right]^{r_2}, \quad r_1 \simeq 0.256, \quad r_2 \simeq 0.153 \quad (34)$$

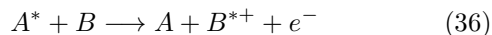
Then the parameter $Qu(A)$ takes the values:

$$0.49, 0.38, 0.35, 0.31, 0.29 \text{ for He, Ne, Ar, Kr and Xe} \quad (35)$$

respectively. The effect of quenching is larger in the case of heavy targets, since, for a given neutrino energy, the energy of the recoiling nucleus is smaller. Thus the number of expected events for Xe assuming a threshold energy of 100 eV is reduced to about 560.

The effect of quenching is exhibited in Fig 11 for the two interesting targets Ar and Xe.

We should mention that it is of paramount importance to experimentally measure the quenching factor. The above estimates were based on the assumption of a pure gas. In our detection scheme the Xe gas carrier (A) is mixed with a small fraction of low ionization potential gas (B). Thus a part of the excitations produced on the Xe atoms could be transferred to ionization through the well known Penning effect as follows:



Such an effect will lead to an increase in the quenching factor and needs to be measured.

VII. CONCLUSIONS

In the present study it has been shown that it is quite simple to detect typical supernova neutrinos in our galaxy, provided that such a supernova explosion takes place (one explosion every 30 years is estimated [31]). The idea is to employ a small size spherical TPC detector filled with a high pressure noble gas. An enhancement of

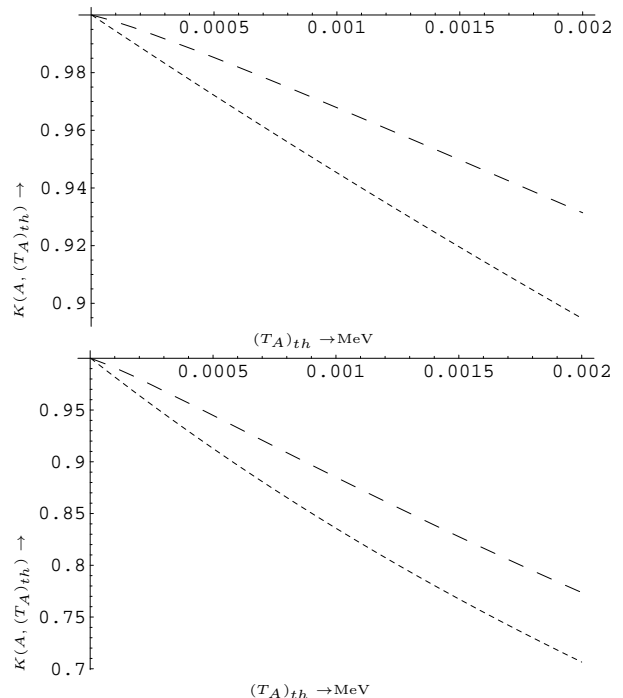


FIG. 11: The function $K(A, (T_A)_{th})$ versus $(T_A)_{th}$ for the target Ar on the top and Xe at the bottom. The short and long dash correspond to no quenching and quenching factor respectively. One sees that the effect of quenching is less pronounced at higher thresholds. The differences appear small, since we present here only the ratio of the rates to that at zero threshold. The effect of quenching at some specific threshold energy is not shown here. For a threshold energy of 100 eV the rates are quenched by factors of 3 and 3.5 for Ar and Xe respectively (see Eq. (35)).

the neutral current component is achieved via the coherent effect of all neutrons in the target. Thus employing, e.g., Xe at 10 Atm, with a feasible threshold energy of about 100 eV in the detection the recoiling nuclei, one expects between 600 and 1900 events, depending on the quenching factor. We believe that networks of such dedicated detectors, made out of simple, robust and cheap technology, can be simply managed by an international scientific consortium and operated by students. This network comprises a system, which can be maintained for several decades (or even centuries). This is a key point towards being able to observe few galactic supernova explosions.

acknowledgments: This work was supported in part by the European Union under the contracts MRTN-CT-2004-503369 and the program PYTHAGORAS-1. The latter is part of the Operational Program for Education and Initial Vocational Training of the Hellenic Ministry of Education under the 3rd Community Support Framework and the European Social Fund. One of the authors (JDV) is indebted for support and hospitality to the NANP05 organizing committee during the NANP05 conference and to Professor Hiroshi Toki of RCNP during

the preparation of the manuscript.

-
- [1] J.F. Beacom, W.M. Farr and P. Vogel, *Phys. Rev D* **66** (2002) 033001;hep-ph/0205220
- [2] J.R. Wilson and R.W.Mayle, *Phys. Rept.* **227** (1993) 97. M. Herant, W. Benz, W.R. Hix, C.L. Fryer and S.A. Golgate, *Astrophys. J.* **435** (1994) 339. M. Rampp and H.T. Janka, *Astrophys. J.* **539** (2000) L33. A. Mezzacappa, M. Liebendorfer, O.E. Messer, W.R. Hix, F.K. Thielemann and S.W. Bruenn, *Phys. Rev. Lett.* **86** (2001) 1935. C.L. Fryer and A. Heger *Astrophys. J.* **541** (2000) 1033. G.G. Raffelt, *Nuc. Phys. Proc. Suppl.* **110** (2002) 254;hep-ph/0201099; R. Tomas, M. Kachelriess, G.G. Raffelt, A.Dighe, A-T Janka and L. Schreck, *JCAP* **0409** (2004) 015; R. Tomas, D. Semikoz, G.G. Raffelt, M. Kachelriess and A.S. Dighe, *Phys. Rev. D* **68** (2002) 093013; M.T. Keil, G.G. Raffelt, A-T Janka, *Astrophys. J.* **590** (2003) 971; J.F. Beacom, R.N. Boyd and A. Mezzacappa, *Phys. Rev. D* **63** (2001) 073011. M.K. Sharp, J.F. Beacom J.A. Formaggio, *Phys. Rev. D* **66** (2002) 013012; hep-ph/0205035. A. Burrows, J. Hayes and B.A. Fryxell, *Astrophys. J.* **450** (1995) 830.
- [3] Y. Fukuda *et al*, The Super-Kamiokande Collaboration, *Phys. Rev. Lett.* **86**, (2001) 5651; *ibid* **81** (1998) 1562 & 1158; *ibid* **82** (1999) 1810 ;*ibid* **85** (2000) 3999.
- [4] Q.R. Ahmad *et al*, The SNO Collaboration, *Phys. Rev. Lett.* **89** (2002) 011302; *ibid* **89** (2002) 011301 ; *ibid* **87** (2001) 071301. K. Lande *et al*, Homestake Collaboration, *Astrophys. J* **496**, (1998) 505 W. Hampel *et al*, The Gallex Collaboration, *Phys. Lett. B* **447**, (1999) 127; J.N. Abdurashitov *et al*, Sage Collaboration, *Phys. Rev. C* **80** (1999) 056801; G.L Fogli *et al*, *Phys. Rev. D* **66** (2002) 053010.
- [5] K. Eguchi *et al*, The KamLAND Collaboration, *Phys. Rev. Lett.* **90** (2003) 021802, hep-exp/0212021. 19
- [6] K. Takahashi, K. Sato, A. Burrows, T. A. Thompson, *Phys.Rev. D* **68** (2003) 113009; hep-ph/0306056
- [7] V. Barger, P. Huber, D. Marfatia, *Phys.Lett. B* **617** (2005) 167. DOI: 10.1016/j.physletb.2005.05.017
- [8] See, e.g, R. Bernabei *et al.*, *Phys. Lett. B* **389** (1996) 757 . R. Bernabei *et al.*, *Phys. Lett. B* **424** (1998) 195; **B** **450** 448 (1999) 448. A. Benoit *et al*, [EDELWEISS collaboration], *Phys. Lett. B* **545** 43 (2002) 43; V. Sanglard *et al* [EDELWEISS collaboration], *Phys. Rev. D* **71** (2005) 122002. D.S. Akerib *et al*, [CDMS Collaboration], *Phys. Rev D* **68** (2003) 082002 ;arXiv:astro-ph/0405033. G. Alner *et al*, (UK Dark Matter Collaboration), *Astropar. Physics* **23** (2005) 444.
- [9] A. Burrows, D. Klein and R. Gandhi, *Phys. Rev. D* **45** (1992) 3361.
- [10] Y. Giomataris and J.D. Vergados, *Nucl. Instr. Meth. A* **530** (2004) 330.
- [11] P. Barbeau, J.I. Collar, J. Miyamoto and I. Shipsey, *IEEE Trans. Nucl. Sci.* **50** (2003) 1285.
- [12] C. Hagmann and A. Bernstein, *IEEE Trans. Nucl. Sci.* **51** (2004) 2151.
- [13] I. Giomataris *et al.*, *Nucl. Instr. Meth. A* **376** (1996) 29
- [14] J.I. Collar and Y. Giomataris, *Nucl. Inst. Meth.* **471** (2001) 254
- [15] P. Gorodetzky *et al.*, *Nucl.Phys.Proc.Suppl.* **138** (2005) 56
- [16] Second workshop on large TPC for low energy rare event detection, 20-21 December 2004, Paris, France.
- [17] C.E. Aalseth *et al.*, *Nucl.Phys.Proc.Suppl.* **110** (2002) 85.
- [18] I. Giomataris *et al.*, hep-ex/0502033. T. Patzak *et al.*, *Nucl. Instr. Meth. A* **434** (1999) 358. B. Ahmed *et al*, *Astropart. Phys.* **19** (2003) 691.
- [19] S. Eidelman *et al* [Particle Data Group], *Phys. Lett. B* **592** (2004) 1.
- [20] M. Hirsch, M.A. Diaz, W. Porod, C. Romao and J,W.F. Valle, *Phys. Rev. D* **62** (2000) 11308-1.
- [21] O. Haug, Amand Faessler, J.D. Vergados and S. Kovalenko, *Nuc. Phys. B*565 (2000) 38; hep-ph/9909318.
- [22]
- [23] ¶.S. Amanic, G.M. Fuller and B. Grstein, *Astropart. Phys.* **24** (2005) 160.
- [24] J. Barranco, O.G. Miranda and T.I. Rashba, Probing new physics with coherent neutrino scattering off nuclei, MPP-2005-85; hep-ph/0508299. P. Vogel and J. Engel, *Phys. Rev. D* **39** (1989) 3378.
- [25] E.A. Paschos and A. Kartavtsev, hep-ph/0309148.
- [26] E. Simon *et al*, *Nucl. Instr. Meth. A* 507 (2003) 643; astro-ph/0212491.
- [27] T. Totani, K. Sato, H.E. Dalhed and J.R. Wilson, *Astrophys.J.* 496 (1998) 216. R. Buras, Hans-Thomas Janka (1), M. Th. Keil , G. G. Raffelt and M. Rampp, *Astrophys.J.* 587 (2003) 320
- [28] J. Lidhart *et al*, *Mat. Phys. Medd. Dan. Vid. Selsk.* **33** (10) (1963) 1
- [29] The NOSTOS experiment and new trends in rare event detection, I. Giomataris *et al*, hep-ex/0502033, submitted to the SIENA2004 International Conference (2005).
- [30] Y. Giomataris, P. Rebourgeard, J.P. Robert, Georges Charpak, *Nucl. Instrum. Meth. A* **376** (1996) 29
- [31] K. Scholberg, *Nucl. Phys. Proc. Suppl.* **91** (2000) 331; hep-ex/0008044.